 doi:10.20944/preprints201801.0159.v1

Article

Development of Piezoelectric Harvesters with Integrated Tuning Devices

Alberto Doria [1,*], Cristian Medè [2], Giulio Fanti [3], Daniele Desideri [4], Alvise Maschio [5], and Federico Moro [6]

[1] Department of Industrial Engineering, University of Padova, Italy; alberto.doria@unipd.it
[2] Department of Industrial Engineering, University of Padova, Italy; cristian.mede@unipd.it
[3] Department of Industrial Engineering, University of Padova, Italy; giulio.fanti@unipd.it
[4] Department of Industrial Engineering, University of Padova, Italy; daniele.desideri@unipd.it
[5] Department of Industrial Engineering, University of Padova, Italy; alvise.maschio@unipd.it
[6] Department of Industrial Engineering, University of Padova, Italy; federico.moro@unipd.it
* Correspondence: alberto.doria@unipd.it; Tel.: +39-049-827-6803

Featured Application: The research aims to lower the natural frequency and to widen the band of operation of piezoelectric harvesters by means of tuning devices integrated with the structural layer of the harvester.

Abstract: The possibility of improving the performance of a piezoelectric harvester by means of novel tuning devices integrated with the harvester's structure is investigated. Some prototypes of harvesters with tuning devices are developed by mounting cantilever dynamic absorbers on standard harvesters. A mathematical model is used for predicting the natural frequencies of the coupled system. Tests on prototypes are carried out with an impulsive method. Experimental results show that a small tuning device can lower the main resonance frequency of a piezoelectric harvester of the same extent as a larger tip mass and moreover generates at high frequency a second resonance peak. A multi-physics numerical model is developed for predicting the generated power and for performing stress-strain analysis of harvesters equipped with Integrated Tuning Devices (ITDs). The numerical model is validated on the basis of experimental results. Several configurations of ITDs are conceived and studied. Numerical results show that harvesters with ITDs are able to generate relevant power at two frequencies owing to the particular shape of the modes of vibration. The stress in the harvesters with ITDs is smaller than the stress in the harvester with a tip mass tuned to the same frequency.

Keywords: harvester; piezoelectric; dynamic vibration absorber; tuning.

1. Introduction

In recent years there has been a great development of energy harvesting techniques based on piezoelectric devices. Piezoelectric harvesters have been successfully used for transforming ambient vibration energy into electrical energy for feeding sensors, biomedical equipment and small electronic devices [1-3]. The tuning of the harvester to the vibration source is essential to improve the vibration-to-electric energy conversion. In the presence of harmonic vibrations optimum tuning is achieved when the natural frequency of the harvester is set equal to vibration frequency [4-5].

Usually cantilever harvesters are tuned by adding a tip mass [5-6], which increases the excitation of the harvester, because the inertia force due to the lumped mass adds to the inertia forces due to the distributed harvester mass. This phenomenon has a beneficial effect on the generated voltage, but it increases the stress inside the harvester, which may be damaged.

The problem of harvester tuning becomes more complex when ambient vibrations are characterized by a variable frequency or by a broadband spectrum. Several techniques have been developed to cope with these working conditions. Some researchers have proposed self-tuning

 doi:10.20944/preprints201801.0159.v1

harvesters [7]. Other researchers have developed wideband harvesters making use of non-linear effects [8-9]. The possibility of widening the band of the harvester by increasing the number of degrees of freedom (DOFs) has been analyzed in some researches [4], in particular in [10-11] two DOFs harvesters have been developed connecting cantilever harvesters with tip masses. Other researchers have analyzed the possibility of exploiting several modes of vibration of the harvester making use of segmented electrodes [12].

The problems of tuning and increasing the bandwidth of a piezoelectric harvester can be tackled by coupling the harvester with a lumped spring-mass system. This technique has been used both in the field of vibrations control and in the field of acoustics. In the former case the added system is named Dynamic Vibration Absorber (DVA) [13]. Since the beginning of 20th century DVAs have been successfully used for controlling vibrations of many mechanical systems including crankshafts, pipes, ships, engines and machine tools [14]. In the field of acoustics the added system is named Helmholtz resonator [15] and it has been used in mufflers [16] and cavities [17].

In the field of energy harvesting several studies have been already carried out. For example [18] in 2005 proposed to attach lead zirconate/lead titanate (PZT) patches (which harvest energy from vibrations) to an auxiliary structure that acts as a DVA for the main vibrating structure. Several researchers studied dynamic magnifiers, which are spring-mass systems placed between the harvester and the moving base [19]. In [20] the dynamic magnifier was added to a piezoelectric stack harvester and the natural frequency of the dynamic magnifier was set equal to the one of the harvester. Numerical results showed the appearance of two resonance peaks, a large increment in the generated power and a significant widening of the bandwidth of the harvester. In [21] the concept of dynamic magnifier was applied to cantilever harvesters. In [22] a cantilever harvester with tip mass was mounted on a supporting beam for lowering the first natural frequency of the integrated system.

These concepts were further extended in [23], where all the modes of a cantilever harvester were tuned to those of a continuous (beam-type) auxiliary structure. Experimental results showed a doubling of resonance peaks in a wide frequency band.

A double-mode harvester was developed in [24]. In this case the harvester does not behave like a DVA, but a DVA, composed of a mass and two helicoidal springs, is used for tuning the harvester and for making possible the exploitation of two modes of vibration. A distributed-parameter model and an experiment showed the potentialities of this harvester.

A DVA composed of a cantilever beam and a tip mass is more suited to integration with an harvester than a DVA composed of a helicoidal spring and tip mass.

This research focuses on piezoelectric harvesters having a multi-layer structure with one or more active layers surrounded by layers of structural, conductive and insulating materials. In these harvesters the structural layer (steel or plastic material) can be extended and shaped to create a DVA, which is named Integrated Tuning Device (ITD). In a simple ITD the structural layer is extended to create a narrow appendix with a final widening: the narrow appendix behaves as a cantilever beam, whereas the final widening behaves as a tip mass. Many alternative designs are possible in order to shape the extension of the structural layer in such a way that a part behaves essentially as a beam and another part behaves essentially as a mass.

In order to assess the validity of this concept, some experimental tests were carried out on prototypes made with a simple technology. Results in the frequency domain show that a DVA is able to transform the original resonance peak of the harvester into a pair of new peaks. The former peak has lower frequency than the original peak and is used for tuning the harvester to the main source of vibrations. The latter peak makes it possible to collect a significant amount of energy at high frequency.

In order to extend the analysis, a multi-physics finite element (FE) model was developed in COMSOL and validated by means of experimental results. New harvesters equipped with ITDs were designed and modeled in COMSOL extending and shaping the structural layer of a standard harvester. The potentialities of the harvesters equipped with IDTs were investigated by means of numerical simulations. Numerical results are presented in terms of frequency response functions

Preprints (www.preprints.org) | NOT PEER-REVIEWED | Posted: 17 January 2018 doi:10.20944/preprints201801.0159.v1

(FRFs) of generated voltage, generated power, stress and strain distributions inside the piezoelectric material.

2. Preliminary design

In order to study the effect of the addition of a cantilever DVA to a piezoelectric harvester, some prototypes were designed and built. The starting point was a PPA 1001 harvester built by MIDE. It is a general-purpose unimorph harvester having a rectangular shape (length 41.1 mm, width 20,8 mm) with a PZT 5H piezoelectric layer and a stainless steel structure.

Figure 1 shows that the small cantilever beams of the cantilever DVAs were made using harmonic steel wire (radius $r = 0.15$ mm, density $\rho = 7850$ kg/m^3), this solution allowed to obtain a low damped structure. The mass elements were small brass discs, whose masses were measured by means of an analytical balance having a resolution of 0.1 mg.

The cantilever DVAs were connected to the free end of the harvester with a removable connection using wax for accelerometers. In some tests the cantilever DVA was joined to the harvester using epoxy adhesive. No difference was found between the results obtained with the two joining techniques.

A lumped-element approach was adopted for tuning the cantilever DVA (having stiffness k_a and equivalent mass m_{eq}) to first natural frequency of the PPA 1001 harvester (f_n):

$$\omega_n = 2\pi f_n = \sqrt{\frac{k_a}{m_{eq}}} \tag{1}$$

Stiffness k_a depends on cantilever length L_a, Young modulus E and moment of inertia I of the wire cross-section:

$$k_a = \frac{3EI}{{L_a}^3} \tag{2}$$

Equivalent mass accounts for the lumped tip mass m_a and a fraction of the mass of the wire (having density ρ) making use of the Rayleigh method [13]:

$$m_{eq} = m_a + \frac{33}{140}\rho\pi r^2 L_a \tag{3}$$

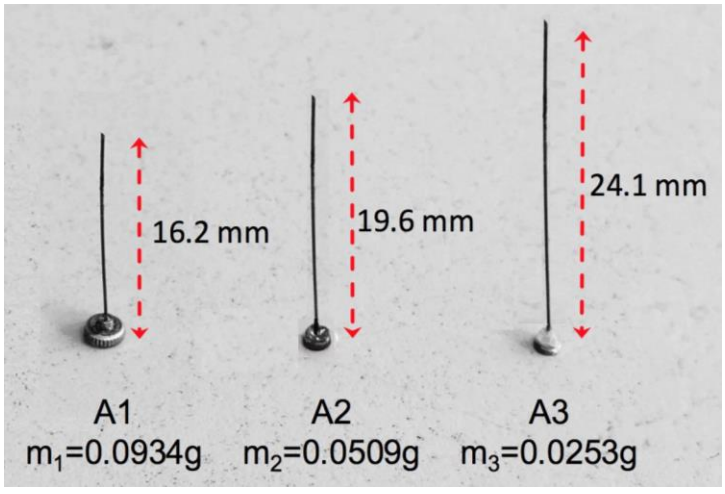

Figure 1. Cantilever DVA for harvesters.

Equations (1), (2) and (3) show that it is possible to tune a cantilever DVA with assigned tip mass m_a and wire radius r by varying the length (L_a) of the cantilever beam. It is well known from the theory of DVA [13] that an increment in the tip mass (m_a) widens the frequency band including the resonance peaks that substitute for the original resonance peak. Therefore, three

Preprints (www.preprints.org) | NOT PEER-REVIEWED | Posted: 17 January 2018 doi:10.20944/preprints201801.0159.v1

different cantilever DVA tuned to the same frequency (f_n = 125 Hz) but with different tip masses were developed.

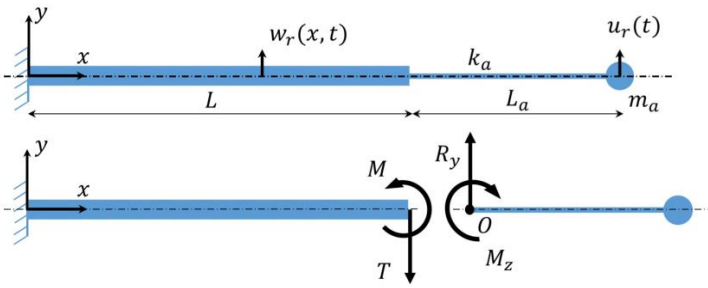

Figure 2. Model of the coupled system.

A simple mathematical model able to predict the natural frequencies of the harvester with cantilever DVA is an useful design tool. The mechanical model represented in Figure 2 was developed, in which the harvester is modeled as a distributed-parameter system and the cantilever DVA as a lumped-element device; $w_r(x,t)$ is the displacement of any point x along the harvester axis in the transverse direction (y) with respect to the base, $u_r(t)$ is the displacement of the mass of the cantilever DVA with respect to the harvester tip ($w_r(L,t)$). The coupling between the mechanical system and the piezoelectric system is neglected, because this phenomenon has a negligible effect on the natural frequencies [4, 12, 24]. The basic equation of the harvester is:

$$(EI)_{eq}\frac{\partial^4 w_r(x,t)}{\partial x^4} + m\frac{\partial^2 w_r(x,t)}{\partial t^2} = 0 \quad (4)$$

$(EI)_{eq}$ is the equivalent bending stiffness of the composite cross-section and m is the mass per unit length of the harvester. From $w_r(x,t)$ bending moment and shear force can be calculated. Equation (4) is solved using the technique of separation of variables [13]:

$$w_r(x,t) = f(t)g(x) \quad (5)$$

$f(t)$ is an harmonic function with frequency ω and $g(x)$ contains both harmonic and exponential terms.

The equation of motion of the DVA is:

$$m_{eq}\left(\frac{d^2 u_r(t)}{dt^2} + \frac{\partial^2 w_r(L,t)}{\partial t^2}\right) = -k_a u_r(t) \quad (6)$$

If an harmonic solution with the same time function of the harvester is considered:

$$u_r(t) = u_{r0} f(t) \quad (7)$$

a relation between DVA displacement amplitude u_{r0} and displacement of the harvester tip $g(L)$ can be found:

$$u_{r0} = \omega^2 \frac{m_{eq} g(L)}{k_a - m_{eq}\omega^2} \quad (8)$$

The natural frequencies of the coupled system can be found by imposing the boundary conditions for the harvester. At the clamped end, the boundary conditions are zero deflection and slope. The boundary conditions for $x = L$ depend on the dynamics of the DVA. Shear force has to be equal to the inertia force of the harvester mass and bending moment has to be equal to the moment of inertia force around point O in Figure 2.

Calculations were performed numerically and results are summarized in Table 1. This table shows that, when the most massive DVA (A1) is added to the harvester, the original natural frequency (125 Hz) is substituted by two new natural frequencies at 98.5 and 156.6 Hz, the bandwidth between the two resonances is 58.1 Hz. If the harvester mass is reduced, the bandwidth between the two resonances decreases.

 doi:10.20944/preprints201801.0159.v1

Table 1. Properties and calculated frequencies of the cantilever DVAs.

DVA	Mass [g]	Length [mm]	f_n[Hz]	f_1[Hz]	f_2[Hz]	Δf[Hz]
A1	0.0934	16.2	125	98.5	156.6	58.1
A2	0.0509	19.6	125	103.9	149.9	46.0
A3	0.0253	24.1	125	108.4	143.7	35.3

3. Experimental tests and results

A specific test rig was developed to excite a small harvester equipped with a cantilever DVA by means of a hammer for modal testing. Impulsive excitation instead of shaker excitation was adopted, because the testing equipment is cheaper and allows to obtain the same Frequency Response Functions (FRFs) [25]. The harvester base was clamped at one end of a suspended aluminum bar and the hammer hit was exerted at the opposite end of the bar, see Figure 3. In this way the hammer impact generated longitudinal vibrations inside the bar that in turn generated the base motion of the harvester.

The aluminum bar was suspended from a frame by means of ropes in order to isolate the system from sources of vibrations other than the hammer impact. The pendular motion caused by the ropes showed a natural frequency about 50 times smaller than the expected frequencies of the harvester with DVA and did not influence measurements. The dimensions of the bar were selected to avoid the presence of bending modes of the bar in the range of frequencies of interest.

The measurement system included a piezoelectric accelerometer mounted on the clamped base of the cantilever and a piezoelectric load cell mounted on the head of the hammer for modal testing. The signals of the sensors and the voltage generated by the harvester were acquired by means of a NI 9234 board. Digital signals were analyzed in time and frequency domain by means of NI Signal Express.

Two electrical parameters were measured to evaluate the performance of the harvester. The former is open circuit voltage, which is an important figure for the design of the energy conversion system [26]. The latter is load voltage in the presence of the optimal load resistance [26].

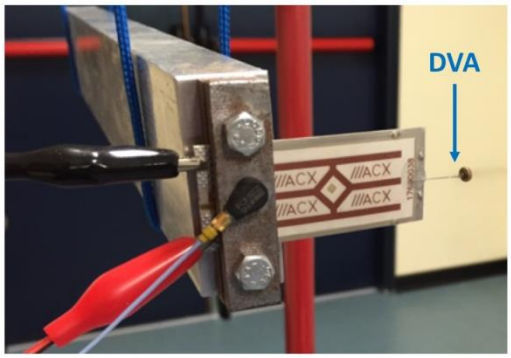

Figure 3. Testing equipment for impulsive testing.

The FRFs between open circuit voltage and base acceleration were measured in order to highlight the effect of the cantilever DVAs on harvester tuning. Five measurements were carried out in each configuration, then the mean values of resonance frequencies and peak amplitudes were calculated.

As regards measurement uncertainty, the repeatability of resonance frequencies resulted about two times the frequency resolution, which is 0.33 Hz. The repeatability of peak amplitudes resulted of about ±5%.

Preprints (www.preprints.org) | NOT PEER-REVIEWED | Posted: 17 January 2018 doi:10.20944/preprints201801.0159.v1

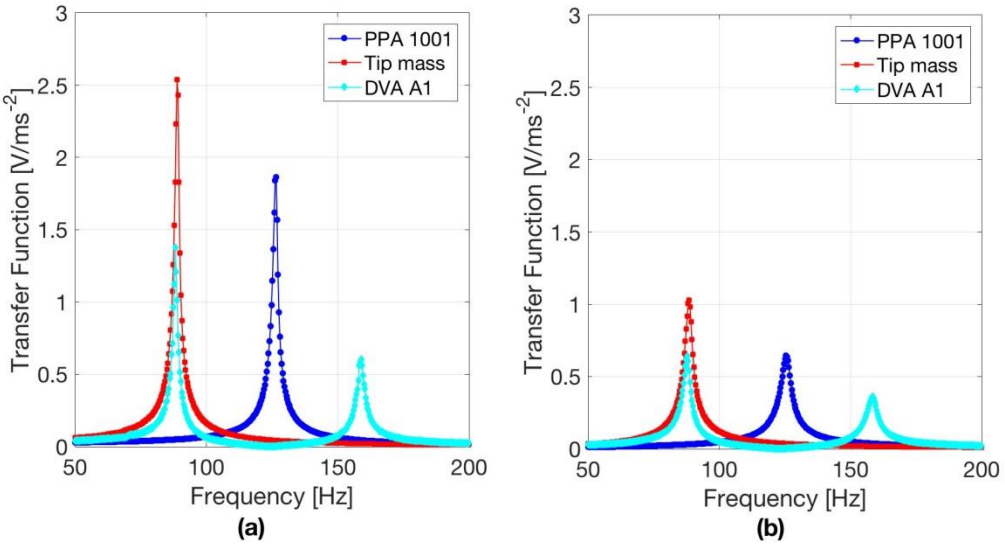

Figure 4. Measured FRFs of the harvester alone, with tip mass and with cantilever DVA. (**a**) Open circuit. (**b**) Optimal load resistance.

Figure 4a shows an example of measured results. Three configurations are considered: harvester PPA 1001 alone, harvester PPA 1001 with DVA A1, harvester PPA1001 with a tip mass.

The introduction of the DVA splits the original resonance peak into two new peaks, the former at lower frequency, the latter at higher frequency. The amplitude of the first new peak is slightly lower than the amplitude of the original peak, but it increases if the mass of the DVA increases, see Table 2. The amplitude of the second new peak is about 1/3 of the one of the original peak and it decreases if the mass of the DVA increases. The frequency interval (Δf) between the two peaks increases when the mass of the DVA increases. The comparison between Table 1 and Table 2 highlights that the simple model of section 2 gives only a first approximation of the natural frequencies of the coupled system.

Modal damping was calculated with the half-power-points method [27]. Results, which are summarized in Table 2, highlight that the damping ratio ζ of the first mode of vibration of the coupled system is essentially equal to the one of the fundamental mode of the harvester alone.

The FRFs of Figure 4a show that the cantilever DVA generates two modes of the harvester that can be excited by a uniform distribution of base acceleration. The second mode can be exploited if the excitation has a wide frequency bandwidth. Conversely, even if the range of frequency of the FRF is extended, the harvester PPA 1001 alone shows only a very small peak at 763 Hz caused by the excitation of the second bending mode.

From the point of view of tuning, the cantilever DVA is able to lower the frequency of the main resonance peak by some tens of Hz. It should be noted that the same effect of the cantilever DVA can be attained by means of a tip mass. Figure 4a shows that with a tip mass of 0.591 g (much larger than the one of A1) the natural frequency is roughly equal to the first natural frequency of the PPA 1001 equipped with A1. With this solution the generated voltage is larger, but the stress inside the piezoelectric material increases as well.

Table 2. Resonance frequencies of the coupled systems and corresponding amplitudes. Mean values of 5 tests.

Preprints (www.preprints.org) | NOT PEER-REVIEWED | Posted: 17 January 2018 doi:10.20944/preprints201801.0159.v1

Harvester	1st Mode			2nd Mode			ΔF [Hz]
	Frequency f_1 [Hz]	Peak amplitude [V/ms^{-2})]	Damping Ratio ζ	Frequency f_2 [Hz]	Peak amplitude [V/ ms^{-2}]	Damping Ratio ζ	
PPA 1001	126.4	1.85	0.0072	-	-	-	-
PPA1001 + Tip Mass	90.0	2.48	0.0087	-	-	-	-
PPA1001 + A1	88.2	1.35	0.0087	158.9	0.55	0.0085	70.7
PPA1001 + A2	93.2	1.33	0.0080	156.4	0.61	0.0077	63.2
PPA1001 + A3	97.4	1.25	0.0073	148.3	0.79	0.0071	50.9

The same series of measurements was carried out considering for each harvester configuration the optimal load resistance [26] for the first resonance peak at frequency ω_r:

$$R_{opt} = \frac{1}{\omega_r C_{pu}} \quad (9)$$

In equation (9) C_{pu} is the capacitance of the harvester. Figure 4b shows an example of experimental results. In all the cases here considered the amplitudes in resonance are significantly lower than the ones in open circuit condition due to the effect of the resistance [5]. The resonance frequency of PPA 1001 and of PPA 1001 with tip mass slightly decreases passing from the open circuit condition to the optimal resistance condition; this result is in agreement with [5] and [28]. In the harvester equipped with DVA the introduction of the optimal resistance lowers the frequency of first resonance peak by about 1 Hz and has a very small effect on the frequency of the second peak. Hence, the frequency shifts caused by the cantilever DVAs in the presence of optimal load are similar to those of Table 2.

The power (P) generated by the harvester in resonance can be calculated from the voltage (V_L) measured in loaded condition:

$$P = \frac{V_L^2}{2R_{opt}} = \frac{|FRF_L|^2 acc^2}{2R_{opt}} \quad (10)$$

FRF_L is the FRF measured in loaded condition, and acc the amplitude of base acceleration.

If the base acceleration is set to 10 m/s², Harvester PPA 1001 generates in resonance 1.61 mW, whereas harvester PPA 1001 with A1 generates 0.97 mW at the first resonance and 0.37 mW at the second resonance.

4. Numerical model and validation

The PPA 1001 unimorph cantilever is composed of 5 layers of different materials, see Figure 5. The active layer is made of PZT 5H (0.15 mm), it is partially covered by a copper electrode (0.03 mm) and by a polyester layer (0.05 mm). The structure is an AISI 304 stainless steel layer (0.15 mm), the bottom layer is made of polymide (0.03 mm).

A numerical FE model was developed with the COMSOL software. The piezoelectric material was modeled as transversely isotropic linear elastic material with polarization axis perpendicular to the layer. The other materials were simulated as linear elastic materials with isotropic properties. The characteristics of the harvester's materials can be found in [29]. A mapped mesh of second order hexahedral elements with 27 nodes was used. The piezoelectric layer was modeled by means of 5 elements in the thickness direction and by 30 elements and 10 elements in the direction of length and width respectively. Geometrical details, like the edges of structural material that surround the piezoelectric material, were taken into account.

Preprints (www.preprints.org) | NOT PEER-REVIEWED | Posted: 17 January 2018 doi:10.20944/preprints201801.0159.v1

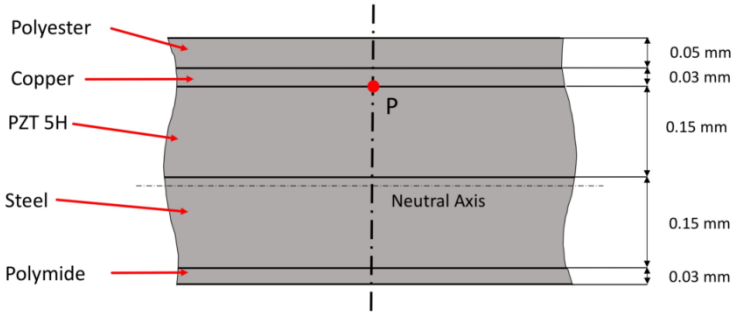

Figure 5. Layers of PPA 1001.

The steady-state harmonic response was calculated in the multi-physics domain, which includes mechanical, electrostatic and electrical equations. In the simulations a hysteretic damping model with $\eta=2\zeta=0.017$ (where ζ is damping ratio) was used, in agreement with experimental results of Table 2.

First the numerical model was validated comparing the numerical FRFs between generated voltage and base acceleration with the experimental FRFs. Both open circuit condition and optimal load resistance were considered.

Figure 6 shows very small differences both in the values of the resonance frequency and in the values of the resonance peak. In open circuit condition the numerical resonance peak is 1.82 V/ms^{-2} and takes place at 125.6 Hz, the experimental values being 1.85 V/ms^{-2} at 126.4 Hz. With optimal load resistance (12.7 kΩ) the numerical resonance peak is 0.60 V/ms^{-2} and takes place at 124.5 Hz, the experimental values being 0.64 V/ms^{-2} at 125.58 Hz.

Then, the numerical model was extended in order to allow the simulation of the harvester equipped with DVA A1. The steel wire of A1 was simulated by a beam of hexahedral elements and the brass disk was simulated by a lumped mass.

Figure 7 shows both the numerical and experimental FRFs between generated voltage and base acceleration of PPA 1001 equipped with A1. In open circuit condition there is a small difference (about 7 %) in the height of the first resonance peak. With optimal load resistance the differences are smaller.

Numerical simulations made it possible also the calculation of the modes of vibration of the harvester equipped with cantilever DVAs. In the first mode of vibration of the coupled system the harvester has a deformed shape very similar to the one of the first mode of a cantilever beam. The cantilever DVA moves in phase with the harvester and its deformed shape looks like the continuation of the one of the harvester. In the second mode of vibration of the coupled system the cantilever DVA moves in opposition with respect to the tip of the harvester, the harvester has a deformed shape similar to one of the first mode of a cantilever beam but with a different curvature.

Preprints (www.preprints.org) | NOT PEER-REVIEWED | Posted: 17 January 2018 doi:10.20944/preprints201801.0159.v1

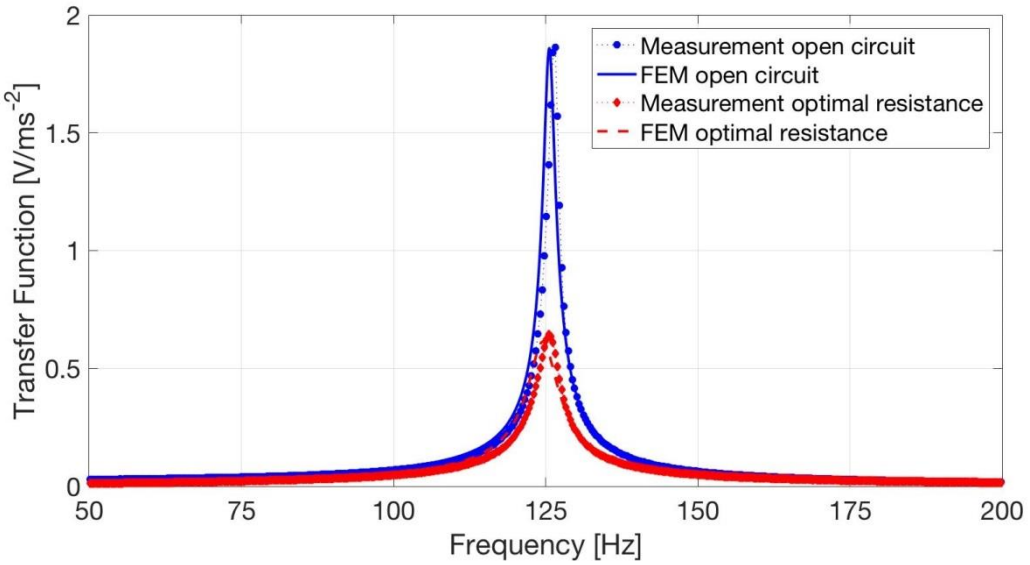

Figure 6. Validation of the numerical model, FRFs of PPA 1001 in open circuit and with optimal load resistance.

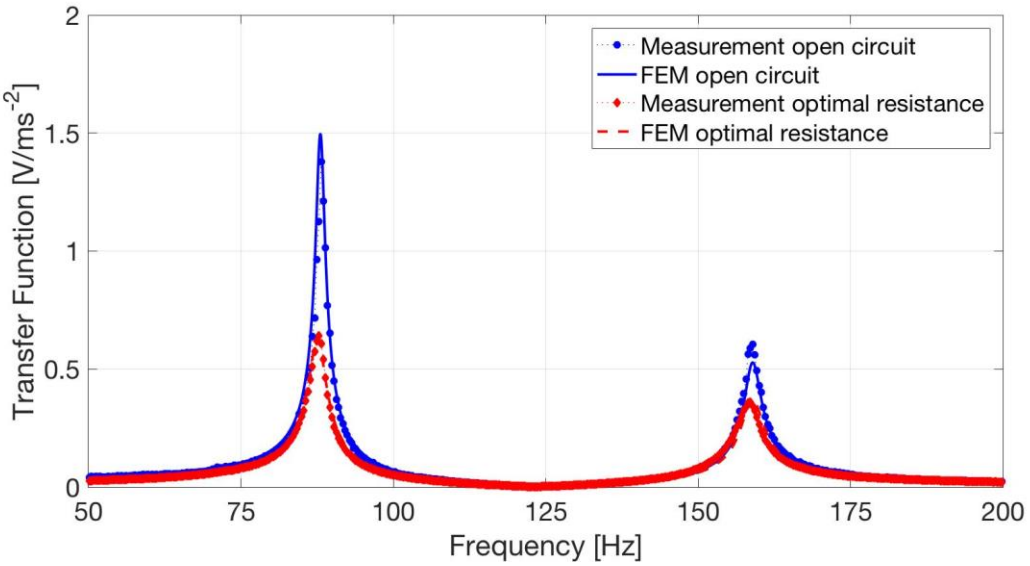

Figure 7. Validation of the numerical model, FRFs of PPA 1001 with A1 in open circuit and with optimal load resistance.

5. Numerical results and discussion

The prototype DVA was built with a simple technology, which is not suited to mass production. After the validation of the numerical model, the FE analysis was used for predicting the performances of tuning devices integrated with the harvester structure (ITDs). The ITDs are built by extending and shaping the structural layer of PPA 1001. The first design, which is named ITD1, is a development of the tested DVA, see Figure 8a. In this case the cantilever beam of the DVA is a narrow extension of the structural layer of the harvester having width b=2.16 mm and length L_a=21.4 mm. The tip mass is a square patch of structural layer having a side length of 6.5 mm, the mass is 0.05 g. Evidently, ITD1 is a 2D structure and the tip mass cannot be considered a point mass, nevertheless Equations (1-3) were used for obtaining a first indication of tuning frequency.

Preprints (www.preprints.org) | NOT PEER-REVIEWED | Posted: 17 January 2018 doi:10.20944/preprints201801.0159.v1

The second design, which is named ITD2, is represented in Figure 8b. In this case the structural layer is extended for 24.5 mm and then a rectangular hole is made. The two lateral sides of the rectangular hole are two cantilever beams whose stiffness (when they bend in parallel) is equal to the stiffness of the cantilever beam of ITD1. The final edge of the rectangular hole is the tip mass, which is equal to the tip mass of ITD1 (0.05 g). It is worth noticing that ITD2 is connected to the harvester in correspondence of the side edges that surround the active area with the PZT layer.

In the following of the paper results dealing with ITD1 and ITD2 are presented, but other kinds of ITDs were conceived and simulated in the framework of this research.

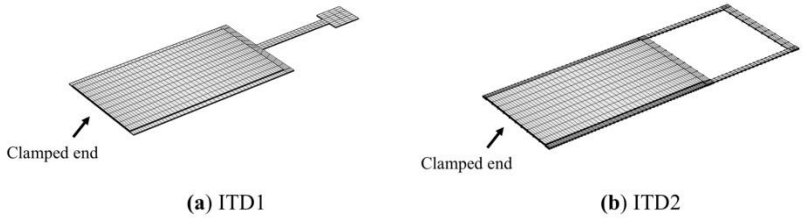

Figure 8. Numerical models of the harvester with. (**a**) ITD1. (**b**) ITD2.

First, the FRFs of the harvesters equipped with ITDs were calculated to assess the tuning capabilities of the ITDs. The open circuit condition was considered, since the resistive load causes only minor frequency shifts of the peaks.

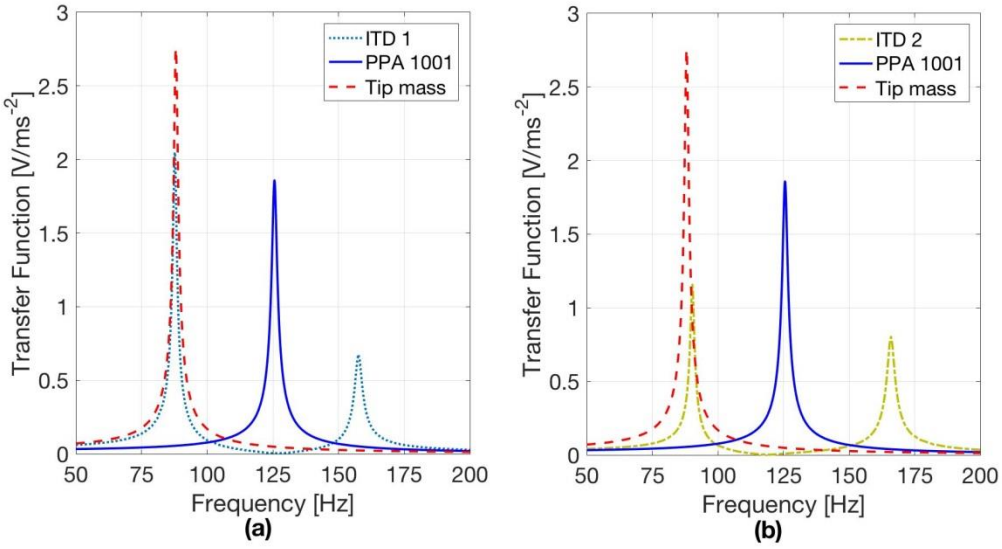

Figure 9. Numerical results, FRFs of the harvester with ITDs, with tip mass and alone; open circuit condition. (**a**) ITD1, (**b**) ITD2.

Figure 9a shows that ITD1 tunes the main resonance to 87.7 Hz with a peak value (2.0 V/ms^{-2}) roughly equal to the one of PPA 1001 alone. The second resonance peak, which appear at 157.5 Hz is much lower than the main peak and is caused by the excitation of the second mode of vibration generated by ITD1. For comparison Figure 9a shows the effect of a large tip mass (0.59 g). In this case the tuning frequency is 88.1 Hz and the peak value is 2.7 V/ms^{-2}.

Figure 9b shows that ITD2 is able to lower the frequency of the main resonance peak to 90.3 Hz. But in this case the heights of the two peaks are more similar and reach values (1.11 V/ms^{-2} and 0.78 V/ms^{-2}) that are about half the value of the resonance peak of PPA 1001 alone (1.81 V/ms^{-2}).

Preprints (www.preprints.org) | NOT PEER-REVIEWED | Posted: 17 January 2018 doi:10.20944/preprints201801.0159.v1

This behavior can be explained looking at the strain distribution inside the PZT layer when the frequency of base excitation coincides with one of the resonance frequencies and the deformed shape is dominated by the mode of vibration excited in resonance.

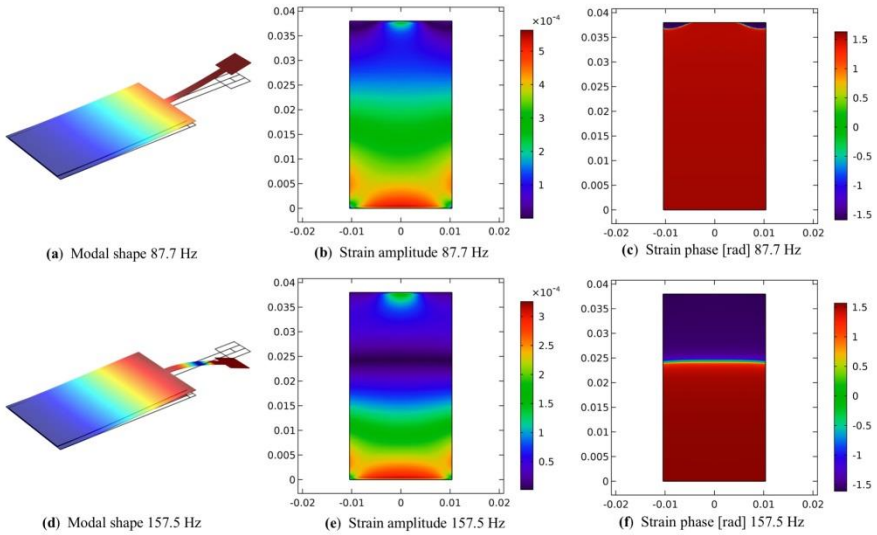

Figure 10. Numerical results, strains in the piezo layer of the harvester with ITD1. (**a**) modal shape at the first resonance (87.7 Hz). (**b**) strain modulus at the first resonance (87.7 Hz). (**c**) strain phase at the first resonance (87.7 Hz). (**d**) Modal shape at the second resonance (157.5 Hz). (**e**) strain modulus at the second resonance (157.5 Hz). (**f**) strain phase at the second resonance (157.5 Hz).

Figure 10 shows the strain in the middle plane of the PZT layer of the harvester equipped with ITD1. This active layer is surrounded by edges of structural material. The strain component in the longitudinal direction is represented, since it is the most important strain component caused by harvester bending. The color maps show both the amplitude and phase of strain. Strain node lines [28], which are the lines on the surface of the PZT layer where the strain changes sign, are represented by light lines in the phase plots.

At the first resonance the ITD moves in phase with the harvester. The amplitude of strain decreases rather regularly from the clamped-end to the free-end. There are changes in the sign of strain near the corners of the free-end of the layer. This is a 3D effect, since the ITD is attached at the middle of the free-end of the harvester, see Figure 8a. With this strain distribution cancellations in generated voltage [28] are very small and the first peak is high. At the second resonance the ITD moves in phase opposition with respect to the harvester tip, see Figure 10d. The strain distribution in this condition is very different with a strain node line at about 6/10 of the harvester's length. There are large cancellations in the generated voltage, which lead to a small resonance peak.

The strain distributions in the PZT layer of the harvester equipped with ITD2 are represented in Figure 11. At the first resonance there is only a strain node line near the central part of the free-end of the layer, because the ITD is attached to the harvester in correspondence of the side edges of structural material that surround the active layer, see Figure 11a. Owing to the presence of this strain node line, a cancellation in the generated voltage takes place, but this effect is small, because the negative strain area is small and negative strains have small amplitudes. When the harvester with ITD2 is excited at the frequency of the second resonance peak, the side beams of ITD2 alter the strain distribution inside the PZT layer less than the central beam of ITD1. There is a strain node at about 7/10 of the harvester's length. Globally, the cancellations due to the change in the sign of strain are small, because negative strains are small and appear in a small part of the PZT layer. The generated voltage is only slightly lower than the one generated at the first resonance.

Preprints (www.preprints.org) | NOT PEER-REVIEWED | Posted: 17 January 2018 doi:10.20944/preprints201801.0159.v1

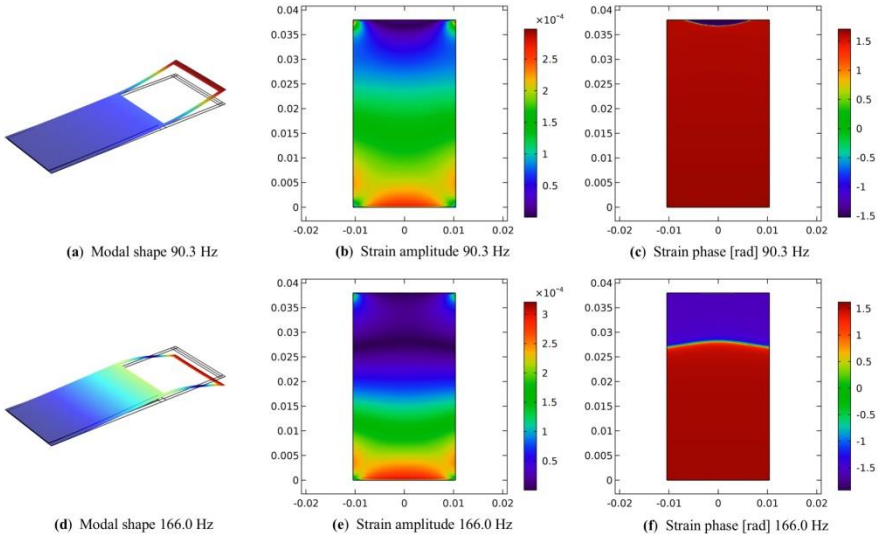

Figure 11. Numerical results, strains in the piezo layer of the harvester with ITD2. (**a**) modal shape at the first resonance (90.3 Hz). (**b**) strain modulus at the first resonance (90.3 Hz). (**c**) strain phase at the first resonance (90.3 Hz). (**d**) modal shape at the second resonance (166.0 Hz). (**e**) strain modulus at the second resonance (166.0 Hz). (**f**) strain phase at the second resonance (166.0 Hz).

The most important characteristic of a piezoelectric harvester is the power that it can generate at the various frequencies. In order to calculate the generated power, load resistance was set equal to the optimal value for the first resonance peak (Equation (9)). The harmonic response with a base acceleration of 10 ms^{-2} was simulated. Calculated results are represented in Figure 12 and the powers generated by the harvesters with ITDs are compared with the powers generated by the harvester alone and by the harvester with a tip mass that tunes the harvester to the same frequency.

The power generated by the harvester with ITD1 at the low frequency resonance (87.0 Hz) is 0.90 mW. This value is lower than the power generated by PPA 1001 alone at 124.6 Hz, but the harvester with ITD1 moreover generates 0.44 mW in correspondence of the high frequency resonance (157.7 Hz).

The harvester with ITD2 appears suited to operate in the presence of wideband excitation or in the presence of a source of excitation with variable frequency, because it generates relevant powers both at the low frequency resonance (0.69 mW at 89.8 Hz) and at the high frequency resonance (0.61 mW at 165.5 Hz). Finally, the harvester with tip mass generates the largest power at 87.3 Hz, but also the stress may be very large due to the increased inertia force.

Preprints (www.preprints.org) | NOT PEER-REVIEWED | Posted: 17 January 2018 doi:10.20944/preprints201801.0159.v1

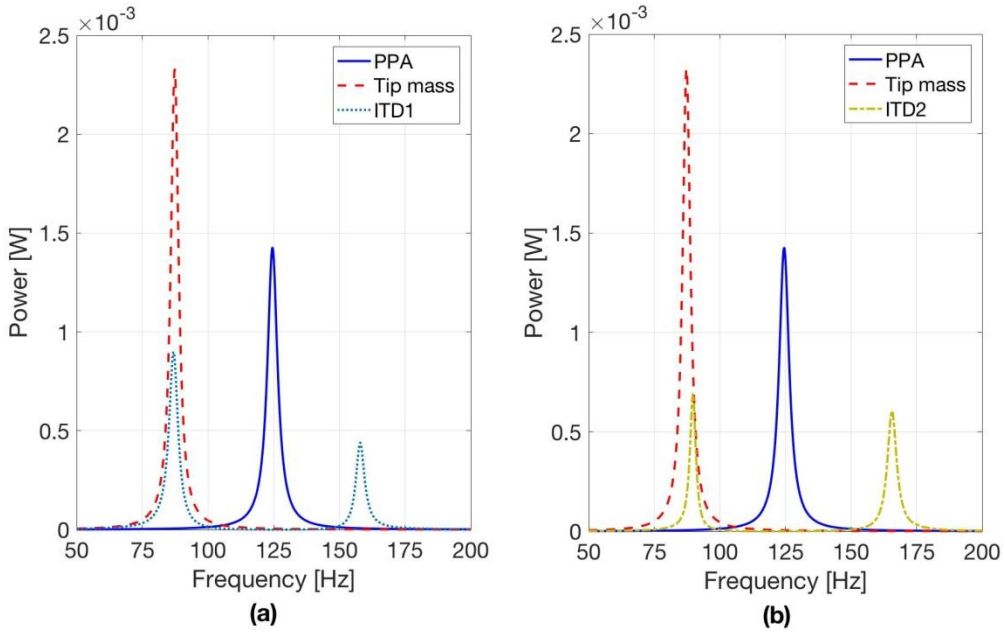

Figure 12. Numerical results, power generated by PPA 1001 equipped with tuning devices, optimal load resistance, base acceleration 10 ms^{-2}(1g). (**a**) ITD1, (**b**) ITD2.

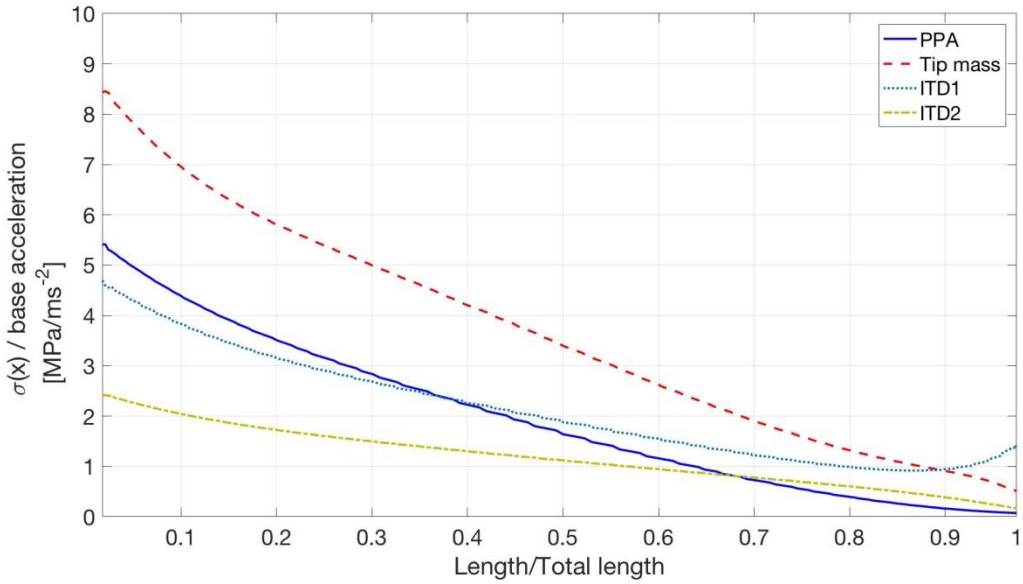

Figure 13. Numerical results, maximum stress in the piezoelectric layer of the harvesters.

The last numerical analysis here presented deals with the stress analysis inside the piezoelectric material. Four configurations were considered: harvesters equipped with ITD1 and ITD2, PPA 1001 alone and with tip mass. The harvesters were excited by a base acceleration of 1 ms^{-2} at the main resonance frequency, which coincides with the low frequency peak of the harvesters with ITDs and with the main peak of the others.

Normal stress in the longitudinal direction σ_x was calculated, which is the most important stress component caused by harvester bending. Stress σ_x was evaluated along the center-line of the upper surface of the PZT layer, which is at the largest distance from the neutral axis of the composite cross-section. Point P of Figure 5 is the trace of this line.

 doi:10.20944/preprints201801.0159.v1

Results are presented in terms of ratio between stress and base acceleration, this figure holds true as far as the harvester has a linear behavior. Figure 13 shows that the introduction of the tip mass does not considerably modify the trend of stress distribution along the span of the harvester, which is characterized by the largest values near the clamp. But the tip mass leads to a large increase in the values, which almost double. Conversely, when ITD1 is introduced, the trend of stress distribution along the span of the harvester changes. In particular, the stress decreases less when moving from the clamp to the tip of the harvester and it increases sharply in the proximity of the connection with the ITD. The maximum value is reached at the clamp and it is similar to the one of PPA 1001 alone. The insertion of ITD2 lowers the stress at the clamped-end more than the insertion of ITD1, this phenomenon is related with the reduced height of the first resonance peak. With ITD2 the stress near the free-end of the PZT layer increases less than with ITD1, since ITD2 is connected to the harvester in correspondence of the side edges of the structural layer that surround the PZT layer, see Figure 8b.

It should be noted that the bending braking strength of PZT 5H is in the range 100 - 140 MPa [30-31] and it considerably reduces in the presence of cyclic loading (see Figure 3 of [31]). Hence, with high acceleration levels the harvester with tip mass may be closer to the failure condition than the harvester with ITDs.

6. Conclusion

Experimental results show that it is possible to develop cantilever DVAs that behave as reactive mechanical loads and are able to modify the natural frequencies and modes of vibration of the harvester, without increasing the damping of the system.

Usually vibration energy is available at frequencies lower than the fundamental frequency of a piezoelectric harvester. Experimental results show that decrements in the fundamental frequency of about 30% can be achieved by means of a simple cantilever DVA.

These concepts, which have been validated by means of prototypes built with a simple technology, are then extended to develop the ITDs. The integration of the tuning device with the structural layer of the harvester is a promising technology, since the extension of the structural layer (steel or plastic material) is rather inexpensive and the extension can be cut into the desired shape by means of consolidated technologies such as punching or laser cutting.

In the framework of this research the potentialities of harvesters equipped with ITDs have been investigated by means of FE simulation. Numerical results show that the ITD has basically the same properties of the cantilever DVA, but some different designs are possible, which correspond to different properties of the coupled system (harvester with ITD).

The first integrated tuning device (ITD1) is suited to lower the natural frequency of the harvester of about 40 Hz and to collect a relevant amount of power at low frequency (about 0.9 mW). The second integrated tuning device (ITD2) is able to generate two modes of the coupled system without important voltage cancellations due to the presence of strain nodes. Therefore, ITD2 allows the collection of significant power (about 0.7 mW) at two frequencies.

The comparison between a tip mass and an ITD able to tune the harvester to the same frequency highlights that the mass of the ITD is about 8% of the tip mass, therefore inertia forces are smaller. This fact reduces the generated voltage but also the stress inside the piezoelectric layer. Hence, an ITD is useful for tuning an harvester when vibration levels are high and stress inside an harvester equipped with a tip mass could reach dangerous values.

The main limit of an ITD seems the increased length of the device, but this limit could be overcome with a folded design in which the mass (sustained by two side beams like in ITD2) lies near the harvester base.

Future research directions are the testing of harvesters with ITDs and the numerical simulation of harvesters equipped with more complex ITDs, which behave as dynamic systems with two or more DOFs.

Acknowledgments: The research was funded by University of Padova grant CPDA142798.

Author Contributions: A. Doria with the contribution of G. Fanti and C. Medè conceived the tuning devices; A. Doria and C. Medè performed the experiments; C. Medè performed the simulations with the supervision of F. Moro; all the authors analyzed and discussed the results, and revised the paper written by A. Doria.

Conflicts of Interest: The authors declare no conflict of interest.

References

1. Cook-Chennault, K. S., Thambi N., Sastry A. M. Powering MEMS portable devices—a review of non-regenerative and regenerative power supply systems with special emphasis on piezoelectric energy harvesting systems. *Smart Mater. Struct*. **2008**, *Vol. 17(4)*, pp. 043001, DOI: 10.1088/0964-1726/17/4/043001.
2. Erturk, A., Inman, D., J. *Piezoelectric Energy Harvesting*; John Wiley & Sons, New York, 2011, ISBN: 978-0-470-68254-8.
3. Anton, S. R., Sodano, H. A. A review of power harvesting using piezoelectric materials (2003–2006). *Smart Mater. Struct.* **2007**, *Vol. 16(3)*, pp. R1-R21, DOI: 10.1088/0964-1726/16/3/R01.
4. Kaźmierski, T. J., Beeby, S. *Energy Harvesting Systems: Principles, Modeling and Applications*; Springer, New York, 2011, ISBN 978-1-4419-7565-2.
5. Priya, S., Inman, D. J. *Energy harvesting technologies*; Springer, New York, 2009, ISBN 978-0-387-76463-4.
6. Erturk, A., Inman, D. J. An experimentally validated bimorph cantilever model for piezoelectric energy harvesting from base excitations. *Smart Mater. Struct.* **2009**, *Vol. 18(2)*, pp. 025009, DOI: 10.1088/0964-1726/18/2/025009
7. Singh, K. B., Bedekar, V., Taheri, S., Priya, S. Piezoelectric vibration energy harvesting system with an adaptive frequency tuning mechanism for intelligent tires, *Mechatronics* **2012**, *Vol. 22(7)*, pp. 970–988, DOI: 10.1016/j.mechatronics.2012.06.006
8. Ramlan, R., Brennan, M. J., Mace, B. R., Burrow, S. G. On the performance of a dual-mode non -linear vibration energy harvesting device. *Journal of Intelligent Material Systems and Structures* **2012**, *Vol. 23(13)*, pp. 1423–1432, DOI: 10.1177/1045389X12443017.
9. Zhang, J., Kong , L., Zhang, L, Li, F., Zhou, W., Ma, S., Qin, L. A Novel ropes-driven wideband piezoelectric vibration energy harvester, *Appl. Sci.* **2016**, *Vol. 6*, 402; DOI:10.3390/app6120402.
10. Staaf, L. G. H., Köhler, E., Parthasarathy, D., Lundgren, P., Enoksson, P. Modelling and experimental verification of more efficient power harvesting by coupled piezoelectric cantilevers, *Journal of Physics: Conference Series* **2014**, *Vol. 557(1)*, pp. 012098, DOI: 10.1088/1742-6596/557/1/012098.
11. Wu, H.; Tang, L.; Yang, Y.; Soh, C.K. A novel two-degrees-of-freedom piezoelectric energy harvester. *J. Intell. Mater. Syst. Struct.* **2012**, *Vol. 24*, pp. 357–368, DOI: 10.1177/1045389X12457254.
12. Erturk, A., Inman, D. J., On Mechanical Modeling of cantilevered piezoelectric vibration energy harvesting. *Journal of Intelligent Material System and Structures* **2008**, *Vol. 19(11)*, pp. 1311-1325, DOI: 10.1177/1045389X07085639
13. Inman, D., J. *Engineering Vibration*, Second Edition; Prentice Hall, Upper Saddle River NJ, 2001, ISBN 0-13-726142-X.
14. Den Hartog J. P. *Mechanical Vibrations*, fourth edition, McGraw-Hill, New York, 1956, ISBN 070163898.
15. Fahy, F. J., Schofield, C. A note on the interaction between a Helmholtz resonator and an acoustic mode of an enclosure. *Journal of Sound and Vibration* **1980**, *Vol. 61*, pp. 254-267 DOI: 10.1016/0022-460X(80)90383-1.
16. Munjal, M. L. *Acoustics of ducts and mufflers*; John Wiley & Sons, New York, 1987, ISBN 0-471-84738-0.
17. Doria, A. A simple method for the analysis of deep cavity and long neck acoustic resonators. *Journal of Sound and Vibration* **2000**, *Vol. 232(4)*, pp. 823-833, DOI: 10.1006/jsvi.1999.2763
18. Cornwell, P. J., Goethal, J., Kowko, J., Damianakis, M. Enhancing Power Harvesting using a Tuned Auxiliary Structure. *Journal of Intelligent Material Systems and Structures* **2005**, *Vol. 16(10)*, pp. 825-834, DOI: 10.1177/1045389X05055279.
19. Tang, X., Zuo, L. Enhanced vibration energy harvesting using dual-mass system. *Journal of Sound and Vibration* **2011**, *Vol. 330(21)*, pp. 5199-5209, DOI: 10.1016/j.jsv.2011.05.019.
20. Aldraihem, O., Baz, A. Energy Harvester with a Dynamic Magnifer. *Journal of Intelligent Material Systems and Structures* **2011**, *Vol. 22(6)*, pp. 521-530, DOI: 10.1177/1045389X11402706

21. Aladwani, A., Arafa, M., Aldraihem, O., Baz, A. Cantilevered Piezoelectric Energy Harvester with a Dynamic Magnifier. *ASME J. Vib. Acoust*. **2012**, *Vol. 134(3)*, pp. 031004, DOI: 10.1115/1.4005824.
22. Kyung, H, Young-Cheol K., Jae Eun K., A Small-form-factor Piezoelectric vibration energy harvester using a resonant frequency-down conversion. *AIP Advances*, **2014**, *Vol. 4*, 107125, DOI 10.1063/1.4898662.
23. Zhou, W., Penamalli, R. G., Zuo L. An efficient vibration energy harvester with a multi-mode dynamic magnifier. *Smart Mater. Struct.* **2012**, *Vol. 21(1)*, pp. 015014, DOI: 10.1088/0964-1726/21/1/015014.
24. Liu, H., Huang, Z., Xu, T., Chen, D. Enhancing output power of a piezoelectric cantilever energy harvester using an oscillator. *Smart Mater. Struct.* **2012**, *Vol. 21*, pp. 065004, DOI: 10.1088/0964-1726/21/6/065004.
25. Doria, A., Moro, F., Desideri, D., Maschio, A., Zhang, A. An impulsive method for the analysis of piezoelectric energy harvesters for intelligent tires. Proceedings of the ASME 2016 International Design Engineering Technical Conference and Computers and Information in Engineering Conference, IDETC/CIE August 21–24, 2016, Charlotte, United States, Vol. 3, 2016, pp. V003T01A025, DOI: 10.1115/DETC2016-59105.
26. Dicken, J., Mitcheson, P. D., Soianov, I., Yeatman, E. M. Power-extraction circuits for piezoelectric energy harvesters in miniature and low-power applications. *IEEE Transactions on power electronics* **2012**, *Vol. 27(11)*, pp. 4514-4529, DOI: 10.1109/TPEL.2012.2192291.
27. de Silva C., W. *Vibration Fundamental and Practice*, Second Edition; Taylor & Francis, Boca Raton FL, 2007, ISBN: 0-8493-1987-0.
28. Erturk, A., Inman, D. J., A distributed parameter electromechanical model for cantilevered piezoelectric energy harvesters. *ASME Journal of Vibration and Acoustics*, **2008**, *Vol. 130*, pp. 041002-1, DOI: 10.1115/1.2890402
29. Midé Engineering Solutions. Available online: https://www.mide.com.
30. Anton, S. R., Erturk, A., Inman, D. J. Bending Strength of Piezoelectric Ceramics and Single Crystals for Multifunctional Load-Bearing Applications. *IEEE Transactions on Ultrasonics, Ferroelectrics, and Frequency Control* **2012**, *Vol. 59(6)*, pp. 1085-1092, DOI: 0.1109/TUFFC.2012.2299
31. Okayasu, M., Ozeki, G., Mizuno, M. Fatigue failure characteristics of lead zirconate titanate piezoelectric ceramics. *Journal of the European Ceramic Society* **2010**, *Vol. 30*, pp. 713–725, DOI: 10.1016/j.jeurceramsoc.2009.09.014.